

Effects of Co-addition of CuBr₂ and NaCl to CH₃NH₃PbI₃(Cl) Perovskite Solar Cells †

Naoki Ueoka and Takeo Oku *

Department of Materials Science, The University of Shiga Prefecture, 2500 Hassaka, Hikone, Shiga 522-8533, Japan; oh21nueoka@ec.usp.ac.jp

* Correspondence: oku@mat.usp.ac.jp; Tel.: +81-749-28-8368

† Presented at the 2nd International Online-Conference on Nanomaterials, 15–30 November 2020; Available online: <https://iocn2020.sciforum.net/>.

Published: 15 November 2020

Abstract: Effects of co-addition of CuBr₂ and NaCl to CH₃NH₃PbI₃(Cl) perovskite solar cells were investigated on the photovoltaic properties and microstructures. Short-circuit current densities and conversion efficiencies were improved by the simultaneous addition of CuBr₂ and NaCl. In addition, the efficiencies of the devices were maintained even after 10 weeks. The perovskite structure changed from a tetragonal to a cubic system by the addition of Na, which resulted in the improvement in the stabilization of the perovskite crystal.

Keywords: perovskite; solar cells; photovoltaic devices; NaCl; sodium; CuBr₂; copper

1. Introduction

Perovskite solar cells are widely studied, and the partial substitution method with different elements and molecules is often used to improve the properties of perovskite solar cells [1–4]. Organic–inorganic metal halide perovskites have a cubic structure with a general formula ABX₃, where A is an organic cation, B is a divalent metal ion, and X is a halide ion [5]. Doped perovskite structures have been obtained by adding various compounds to the perovskite precursor solutions, and the various dopants investigated are as follows: CH(NH₂)₂²⁺ [6–9], C(NH₂)₃⁺ [10,11], CH₃CH₂NH₃ [12], Cs⁺ [7,13], Rb⁺ [7,14], and K⁺ [15–17] at CH₃NH₃⁺ (MA⁺) sites, Sn²⁺ [18,19] or Sb³⁺ [20,21] at Pb²⁺ sites, and Br[−] and Cl[−] at I[−] sites [22–24].

In previous studies, perovskite crystals have been synthesized from MAPbI_{3-x}Cl_x mixed precursor solutions with MAI and PbCl₂ in the ratio of 3:1 [25–27], and the highest conversion efficiency was obtained for the cells fabricated at 140 °C [26]. Although annealing at high temperatures above 200 °C was possible through the use of polysilanes in chlorobenzene [17,28], perovskite grains may decompose even at 150 °C, and MAPbI₃ changes into PbI₂ by MA desorption. Another approach to improve the MAPbI_{3-x}Cl_x cells is by adding a small amount of excess PbI₂ to the MAPbI_{3-x}Cl_x precursor solutions [29]. The recombination of electrons and holes was suppressed by the formation of a small amount of PbI₂, and the external quantum efficiencies increased. Stabilities of the PbI₂-added cells were also improved [30], and Cl was an important element to improve the stability, which was evidenced by the constant Cl content in the MAPbI_{3-x}Cl cells even after several weeks [29,30].

The short-circuit current density was also increased by the simultaneous addition of alkali metal iodides (NaI, KI, RbI, or CsI) and CuBr₂ to mixed perovskite precursor solutions with MAI, PbCl₂, and PbI₂ [31]. It was suggested that the lattice constant decreased through the addition of CuBr₂ because of the smaller ionic radius of Cu²⁺ compared with that of Pb²⁺. An increase of the density of states owing to the alkali metal elements was confirmed by first-principles calculations, which

contributed to the increase of charge generation by light absorption in the shorter wavelength range compared with the band gap energy of the perovskite. In the co-addition study, it was necessary to optimize the adding amount of CuBr₂ and alkali metal iodides to improve further the photovoltaic characteristics of the perovskite devices. However, increasing the amount of Cu leads to lattice defects that break the bond between Cu/Pb and halogen due to the smaller ionic radius of Cu²⁺ than that of Pb²⁺. The addition of alkali metal elements is effective in stabilizing the perovskite solar cells because of the more stable alkali metal elements compared with MA. Since Cu–Cl bond is shorter than the Cu–Br bond for MA₂CuCl₂Br₂ with two-dimensionality [32], it is considered that the smaller ionic radii such as that of Na/Cl with excellent solubility is effective for the perovskite formation.

The purpose of the present study is to fabricate NaCl/CuBr₂ co-added MAPbI_{3-x}Cl_x photovoltaic devices and to characterize the photovoltaic properties and crystal structures. The additive quantities of NaCl and CuBr₂ to the perovskite precursor solutions are optimized to improve the photovoltaic performance and stability of the perovskite solar cells [33]. Then, the effects of Na addition to Cu-modified perovskite are investigated by analyzing the changes in the conversion efficiencies and the microstructures. The tolerance factor approaches 1 by the introduction of Cu²⁺ at the position of Pb²⁺ because of the smaller ionic radius of Cu²⁺ (0.73 Å) compared with that of Pb²⁺ (1.19 Å), thus a more stable perovskite structure is expected to be formed by the addition of CuBr₂. Gibbs free energies were also calculated and compared.

2. Materials and Methods

A schematic illustration of the present perovskite photovoltaic cells is shown in Figure 1. F-doped tin oxide (FTO) substrates were cleaned in an ultrasonic bath with acetone and methanol and dried under nitrogen gas. The TiO₂ (0.15 and 0.30 M) precursor solutions were prepared from titanium diisopropoxide bis(acetyl acetonate) (Sigma-Aldrich, Tokyo, Japan, 0.055 and 0.11 mL) with 1-butanol (1 mL). The 0.15 M TiO₂ precursor solution was spin-coated on the FTO substrate at 3000 rpm for 30 s, and the coated substrate was then annealed at 125 °C for 5 min. The 0.30 M TiO₂ precursor solution was spin-coated on the TiO₂ layer at 3000 rpm for 30 s, and the resulting substrate was annealed at 125 °C for 5 min. The process to form the 0.30M precursor layer was performed twice. Then, the FTO substrate was sintered at 550 °C for 30 min to form a compact TiO₂ layer [33–35]. To form the mesoporous TiO₂ layer, a TiO₂ paste was prepared from the TiO₂ powder (Aerosil, Tokyo, Japan, P-25) with poly(ethylene glycol) (Nacalai Tesque, Kyoto, Japan, PEG #20000) in ultrapure water. The solution was mixed with acetylacetone (Wako Pure Chemical Industries, Osaka, Japan, 10 mL) and surfactant (Sigma-Aldrich, Triton X-100, 5 mL) for 30 min and then allowed to stand for 24 h to remove bubbles from the solution. Then, the TiO₂ paste was spin-coated on the compact TiO₂ layer at 5000 rpm for 30 s. The resulting cell was heated at 125 °C for 5 min and then annealed at 550 °C for 30 min to form the mesoporous TiO₂ layer.

To prepare the perovskite compounds, mixed solutions of CH₃NH₃I (2.4 M, Showa Chemical, Tokyo, Japan), PbCl₂ (0.8 M, Sigma-Aldrich, St. Louis, MO, USA), and PbI₂ (0.08 M, Sigma-Aldrich) in DMF (Sigma-Aldrich, 500 mL) were prepared for the standard cell [33]. Pb or MA in the perovskite structure was expected to be substituted by Cu or alkali metal elements, respectively. These perovskite solutions were then introduced into the TiO₂ mesopores by spin-coating at 2000 rpm for 60 s, followed by annealing at 140 °C for 10 min under 27 °C and 40% humidity in air.

A hole-transport layer was prepared by spin-coating. A solution of spiro-OMeTAD (Wako Pure Chemical Industries, Osaka, Japan, 50 mg) in chlorobenzene (Wako Pure Chemical Industries, 0.5 mL) was mixed with a solution of lithium bis(tri-fluoromethylsulfonyl)imide (Li-TFSI; Tokyo Chemical Industry, Tokyo, Japan, 260 mg) in acetonitrile (Nacalai Tesque, Kyoto, Japan, 0.5 mL) for 24 h. The former solution with 4-tertbutylpyridine (Sigma-Aldrich, 14.4 mL) was mixed with the Li-TFSI solution (8.8 mL) for 30 min at 70 °C. Then, the spiro-OMeTAD solution was spin-coated on the perovskite layer at 4000 rpm for 30 s. All procedures were performed in ambient air. Finally, gold (Au) electrodes were evaporated as top electrodes using a metal mask for the patterning. Layered structures of the prepared photovoltaic cells are denoted as FTO/TiO₂/perovskite/spiro-

OMeTAD/Au. The prepared perovskite photovoltaic devices were stored at 22 °C and ~30% humidity.

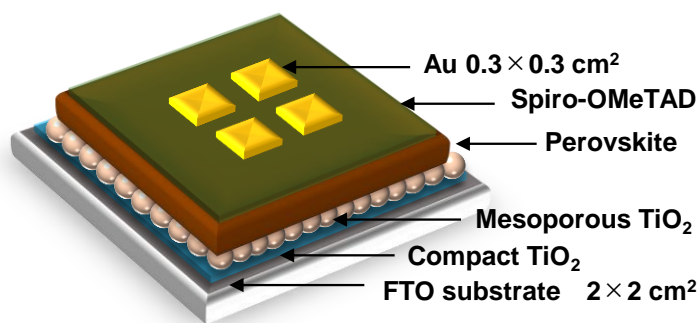


Figure 1. Schematic illustration of the present perovskite photovoltaic devices.

The photovoltaic properties of the fabricated solar cells were investigated by current density–voltage (J – V) characteristics and external quantum efficiency (EQE). Microstructures of the thin films were investigated by X-ray diffraction (XRD), optical microscopy, and scanning electron microscopy (SEM)/energy dispersive spectroscopy (EDS).

3. Results and Discussion

Table 1 shows photovoltaic parameters of the present perovskite photovoltaic devices with added NaCl and CuBr₂ under air mass 1.5 sunlight illumination [33]. The device with only 2% CuBr₂ added without NaCl provided a short-circuit current density (J_{sc}) of 18.9 mA cm⁻², an open-circuit voltage (V_{oc}) of 0.952 V, a fill factor (FF) of 0.655, and a conversion efficiency (η) of 11.8%. The J_{sc} was increased from 18.9 to 22.7 mA cm⁻² by the simultaneous addition of 2% CuBr₂ and 2% NaCl, and the η increased to 14.5%. Hysteresis of the current density–voltage curves were decreased by the co-addition of 2% CuBr₂ and 2% NaCl, which contributed to suppressing the recombination between a hole and an electron. For the 5% CuBr₂-added device, the carrier transport property and the quality of the perovskite layer were improved by increasing the amount of NaCl added, which resulted in an improvement of η .

Stability measurements of the photovoltaic parameters up to 10 weeks were carried out. The η of the (2% NaCl + 2% CuBr₂)-added device remained almost constant for 10 weeks. Although most of Cl were evaporated during the annealing process, a small amount of Cl remained in the perovskite layers. The remained Cl in the perovskite layer would play a critical role in the perovskite grain growth, which resulted in the few defects in perovskite thin films, and also lead to stability. The higher V_{oc} and FF of the (7% CuBr₂ + 5% NaCl)-added device were maintained for 10 weeks in comparison with those of the (5% CuBr₂ + 5% NaCl)-added device, which caused a structural transition from a tetragonal to a cubic system by adding excess CuBr₂, and suppressed recombination between a hole and an electron owing to the pinhole decrease.

Table 1. Measured photovoltaic parameters of the perovskite photovoltaic devices.

Devices	J_{sc} (mA cm ⁻²)	V_{oc} (V)	FF	R_s (Ω cm ²)	R_{sh} (Ω cm ²)	H (%)	η_{ave} (%)
Standard	20.6	0.888	0.628	5.02	2330	11.5	10.8
2% CuBr ₂	18.9	0.952	0.655	6.34	1815	11.8	11.3
2% NaCl	20.9	0.942	0.610	6.93	657	12.0	11.6
2% CuBr ₂ + 2% NaCl	22.7	0.944	0.676	5.93	2567	14.5	13.6

The partial Na would transfer into the MA vacancy site after 10 weeks, which caused the structural transformation from a pseudocubic system to a cubic system, as shown in Figure 2. This structural change indicated that a small amount of Na improved the stability of the photovoltaic

properties. Although the present perovskite structures exhibited an almost cubic structure from the lattice constant, weak diffraction peaks corresponding to tetragonal symmetry were observed at $\sim 23^\circ$, and this structure was classified as pseudocubic [5,36] almost of a/c axis was 1 in the present work. This pseudocubic structure transformed into perfect cubic symmetry by the addition of excess CuBr_2 , which was confirmed by the disappearance of the diffraction peaks at $\sim 23^\circ$ for the 10% CuBr_2 -added devices.

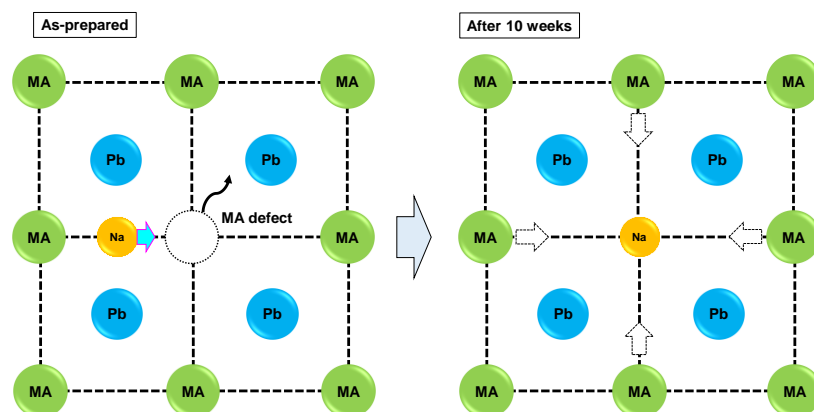


Figure 2. Stability mechanism for the Na-added perovskite crystals.

4. Conclusions

Effects of co-addition of NaCl and CuBr_2 to MAPbI_3 were investigated on the microstructures and photovoltaic properties. A smooth perovskite layer was obtained under the ambient air, and the J_{sc} was improved by the simultaneous addition of CuBr_2 and NaCl . The conversion efficiency of 14% was maintained for the (2% CuBr_2 + 2% NaCl)-added device even after 10 weeks. The perovskite structure changed from a pseudocubic (tetragonal) to a cubic system by the addition of Na . The Na atoms exist at the interstitial sites and are transferred to the MA vacancy sites after several weeks, which resulted in the improvement in the stabilization of the perovskite crystal. The photovoltaic performance of the device co-added with CuBr_2 and NaCl was superior to that of the device added with CuBr_2 and NaI .

Author Contributions: Conceptualization, N.U.; Methodology, N.U. and T.O.; Formal Analysis, N.U. and T.O.; Investigation, N.U.; Resources, N.U. and T.O.; Data Curation, N.U. and T.O.; Writing—Original Draft Preparation, N.U. and T.O.; Project Administration, N.U. and T.O.; Funding Acquisition, N.U. and T.O. All authors have read and agreed to the published version of the manuscript.

Funding: A part of the present study was supported by JSPS KAKENHI Grant Number 19J15017 and the Super Cluster Program of the Japan Science and Technology Agency (JST).

Conflicts of Interest: The authors declare no conflicts of interest.

References

1. Abdi-Jalebi, M.; Andaji-Garmaroudi, Z.; Pearson, A.J.; Divitini, G.; Cacovich, S.; Philippe, B.; Rensmo, H.; Ducati, C.; Friend, R.H.; Stranks, S.D. Potassium- and rubidium-passivated alloyed perovskite films: Optoelectronic properties and moisture stability. *ACS Energy Lett.* **2018**, *3*, 2671–2678, doi:10.1021/acsenerylett.8b01504.
2. Zhao, W.; Yao, Z.; Yu, F.; Yang, D.; Liu, S.F. Alkali metal doping for improved $\text{CH}_3\text{NH}_3\text{PbI}_3$ perovskite solar cells. *Adv. Sci.* **2018**, *5*, 1700131, doi:10.1002/advs.201700131.
3. Zhao, Z.Q.; You, S.; Huang, J.; Yuan, L.; Xiao, Z.Y.; Cao, Y.; Cheng, N.; Hu, L.; Liu, J.F.; Yu, B.H. Molecular modulator for stable inverted planar perovskite solar cells with efficiency enhanced by interface engineering. *J. Mater. Chem. C* **2019**, *7*, 9735–9742, doi:10.1039/C9TC03259B.

4. Lu, Y.A.; Chang, T.H.; Wu, S.H.; Liu, C.C.; Lai, K.W.; Chang, Y.C.; Chang, Y.C.; Lu, H.C.; Chu, C.W.; Ho, K.C. Coral-like perovskite nanostructures for enhanced light-harvesting and accelerated charge extraction in perovskite solar cells. *Nano Energy* **2019**, *58*, 138–146, doi:10.1016/j.nanoen.2019.01.014.
5. Oku, T. Crystal structures of perovskite halide compounds used for solar cells. *Rev. Adv. Mater. Sci.* **2020**, *59*, 264–305, doi:10.1515/rams-2020-0015.
6. Zhao, Y.; Tan, H.; Yuan, H.; Yang, Z.; Fan, J.Z.; Kim, J.; Voznyy, O.; Gong, X.; Quan, L.N.; Tan, C.S.; et al. Perovskite seeding growth of formamidinium-lead-iodide-based perovskites for efficient and stable solar cells. *Nat. Commun.* **2018**, *9*, 1–10, doi:10.1038/s41467-018-04029-7.
7. Philippe, B.; Saliba, M.; Baena, J.-P. C.; Cappel, U.B.; Cruz, S.H. T.; Grätzel, M.; Hagfeldt, A.; Rensmo, H. Chemical distribution of multiple cation (Rb⁺, Cs⁺, MA⁺, and FA⁺) perovskite materials by photoelectron spectroscopy. *Chem. Mater.* **2017**, *29*, 3589–3596, doi:10.1021/acs.chemmater.7b00126.
8. Ono, L.K.; Perez, E.J.J.; Qi, Y. Progress on perovskite materials and solar cells with mixed cations and halide anions. *ACS Appl. Mater. Interfaces* **2017**, *9*, 30197–30246, doi:10.1021/acsami.7b06001.
9. Suzuki, A.; Kato, M.; Ueoka, N.; Oku, T. Additive effect of formamidinium chloride in methylammonium lead halide compound-based perovskite solar cells. *J. Electron. Mater.* **2019**, *48*, 3900–3907, doi:10.1007/s11664-019-07153-2.
10. Jodlowski, A.D.; Roldán-Carmona, C.; Grancini, G.; Salado, M.; Ralaiarisoa, M.; Ahmad, S.; Koch, N.; Camacho, L.; Miguel, G.; Nazeeruddin, M. Large guanidinium cation mixed with methylammonium in lead iodide perovskites for 19% efficient solar cells. *Nat. Energy* **2017**, *2*, 972–979, doi:10.1038/s41560-017-0054-3.
11. Kishimoto, T.; Suzuki, A.; Ueoka, N.; Oku, T. Effects of guanidinium addition to CH₃NH₃PbI_{3-x}Cl_x perovskite photovoltaic devices. *J. Ceram. Soc. Jpn.* **2019**, *127*, 491–497, doi:10.2109/jcersj2.18214.
12. Nishi, K.; Oku, T.; Kishimoto, T.; Ueoka, N.; Suzuki, A. Photovoltaic characteristics of CH₃NH₃PbI₃ perovskite solar cells added with ethylammonium bromide and formamidinium iodide. *Coatings* **2020**, *10*, 410, doi:10.3390/coatings10040410.
13. Singh, R.; Sandh, S.; Yadav, H.; Lee, J.J. Stable triple-cation (Cs⁺-MA⁺-FA⁺) perovskite power formation under ambient conditions for hysteresis-free high-efficiency solar cells. *ACS Appl. Mater. Interfaces* **2019**, *11*, 29941–29949, doi:10.1021/acsami.9b09121.
14. Saliba, M.; Matsui, T.; Domanski, K.; Seo, J.Y.; Ummadisingu, A.; Zakeeruddin, S.M.; Baena, J.P.C.; Tress, W.R.; Abate, A.; Hagfeldt, A.; et al. Incorporation of rubidium cations into perovskite solar cells improves photovoltaic performance. *Science* **2016**, *354*, 206–209, doi:10.1126/science.aah5557.
15. Machiba, H.; Oku, T.; Kishimoto, T.; Ueoka, N.; Suzuki, A. Fabrication and evaluation of K-doped MA_{0.8}FA_{0.1}K_{0.1}PbI₃(Cl) perovskite solar cells. *Chem. Phys. Lett.* **2019**, *730*, 117–123, doi:10.1016/j.cplett.2019.05.050.
16. Kandori, S.; Oku, T.; Nishi, K.; Kishimoto, T.; Ueoka, N.; Suzuki, A. Fabrication and characterization of potassium- and formamidinium-added perovskite solar cells. *J. Ceram. Soc. Jpn.* **2020**, *128*, 805–811, doi:10.2109/jcersj2.20090.
17. Oku, T.; Kandori, S.; Taguchi, M.; Suzuki, A.; Okita, M.; Minami, S.; Fukunishi, S.; Tachikawa, T., Polysilane-inserted methylammonium lead iodide perovskite solar cells doped with formamidinium and potassium. *Energies* **2020**, *13*, 4776, doi:10.3390/en13184776.
18. Tong, J.; Song, Z.; Kim, D.M.; Chen, X.; Chen, C.; Palmstrom, A.F.; Ndione, P.F.; Reese, M.O.; Dunfield, S.P.; Reid, O.G.; et al. Carrier lifetimes of >1 μs in Sn-Pb perovskites enable efficient all-perovskite tandem solar cells. *Science* **2019**, *364*, 475–479, doi:10.1126/science.aav7911.
19. Li, M.; Wang, Z.K.; Zhuo, M.P.; Hu, Y.; Hu, K.H.; Ye, Q.Q.; Jain, S.M.; Yang, Y.G.; Gao, X.Y.; Liao, L.S. Pb-Sn-Cu ternary organometallic halide perovskite solar cells. *Adv. Mater.* **2018**, *30*, 1800258, doi:10.1002/adma.201800258.
20. Oku, T.; Ohishi, Y.; Suzuki, A. Effects of antimony addition to perovskite-type CH₃NH₃PbI₃ photovoltaic devices. *Chem. Lett.* **2016**, *45*, 134–136, doi:10.1246/cl.150984.
21. Oku, T.; Ohishi, Y.; Suzuki, A.; Miyazawa, Y. Effects of Cl addition to Sb-doped perovskite-type CH₃NH₃PbI₃ photovoltaic devices. *Metals* **2016**, *6*, 147, doi:10.3390/met6070147.
22. Shi, D.; Adinolfi, V.; Comin, R.; Yuan, M.; Alarousu, E.; Buin, A.; Chen, Y.; Hoogland, S.; Rothenberger, A.; Katsiev, K.; et al. Low trap-state density and long carrier diffusion in organolead trihalide perovskite single crystals. *Science* **2015**, *347*, 519–522, doi:10.1126/science.aaa2725.

23. Oku, T.; Suzuki, K.; Suzuki, A. Effects of chlorine addition to perovskite-type $\text{CH}_3\text{NH}_3\text{PbI}_3$ photovoltaic devices. *J. Ceram. Soc. Jpn.* **2016**, *124*, 234–238, doi:10.2109/jcersj2.15250.
24. Oku, T.; Ohishi, Y.; Suzuki, A.; Miyazawa, Y. Effects of NH_4Cl addition to perovskite $\text{CH}_3\text{NH}_3\text{PbI}_3$ photovoltaic devices. *J. Ceram. Soc. Jpn.* **2017**, *125*, 303–307, doi:10.2109/jcersj2.16279.
25. Ueoka, N.; Oku, T.; Ohishi, Y.; Tanaka, H.; Suzuki, A. Effects of excess PbI_2 addition to $\text{CH}_3\text{NH}_3\text{PbI}_{3-x}\text{Cl}_x$ perovskite solar cells. *Chem. Lett.* **2018**, *47*, 528–531, doi:10.1246/cl.171214.
26. Oku, T.; Ohishi, Y. Effects of annealing on $\text{CH}_3\text{NH}_3\text{PbI}_3(\text{Cl})$ perovskite photovoltaic devices. *J. Ceram. Soc. Jpn.* **2018**, *126*, 56–60, doi:10.2109/jcersj2.17162.
27. Ueoka, N.; Oku, T.; Suzuki, A.; Sakamoto, H.; Yamada, M.; Minami, S.; Miyauchi, S. Fabrication and characterization of $\text{CH}_3\text{NH}_3(\text{Cs})\text{Pb}(\text{Sn})\text{I}_3(\text{Cl})$ perovskite solar cells with TiO_2 nanoparticle layers. *Jpn. J. Appl. Phys.* **2018**, *57*, 02CE03, doi:10.7567/JJAP.57.02CE03.
28. Taguchi, M.; Suzuki, A.; Oku, T.; Ueoka, N.; Minami, S.; Okita, M. Effects of annealing temperature on decaphenylcyclopentasilane-inserted $\text{CH}_3\text{NH}_3\text{PbI}_3$ perovskite solar cells. *Chem. Phys. Lett.* **2019**, *737*, 136822, doi:10.1016/j.cplett.2019.136822.
29. Ueoka, N.; Oku, T.; Tanaka, H.; Suzuki, A.; Sakamoto, H.; Yamada, M.; Minami, S.; Miyauchi, S.; Tsukada, S. Effects of PbI_2 addition and TiO_2 electron transport layers for perovskite solar cells. *Jpn. J. Appl. Phys.* **2018**, *57*, 08RE05, doi:10.7567/JJAP.57.08RE05.
30. Ueoka, N.; Oku, T. Stability characterization of PbI_2 -added $\text{CH}_3\text{NH}_3\text{PbI}_{3-x}\text{Cl}_x$ photovoltaic devices. *ACS Appl. Mater. Interfaces* **2018**, *10*, 44443–44451, doi:10.1021/acsami.8b16029.
31. Ueoka, N.; Oku, T.; Suzuki, A. Additive effects of alkali metals on Cu-modified $\text{CH}_3\text{NH}_3\text{PbI}_{3-x}\text{Cl}_x$ photovoltaic devices. *RSC Adv.* **2019**, *9*, 24231–24240, doi.org/10.1039/C9RA03068A.
32. Cortecchia, D.; Dewi, H.A.; Yin, J.; Bruno, A.; Chen, S.; Baikie, T.; Boix, P.P.; Grätzel, M.; Mhaisalkar, S.; Soci, C.; et al. Lead-free $\text{MA}_2\text{CuCl}_x\text{Br}_{4-x}$ hybrid perovskites. *Inorg. Chem.* **2016**, *55*, 1044–1052, doi:10.1021/acs.inorgchem.5b01896.
33. Ueoka, N.; Oku, T. Effects of co-addition of sodium chloride and copper(II) bromide to mixed-cation mixed-halide perovskite photovoltaic devices. *ACS Appl. Energy Mater.* **2020**, *3*, 7272–7283, doi:10.1021/acsaem.0c00182.
34. Oku, T.; Zushi, M.; Imanishi, Y.; Suzuki, A.; Suzuki, K. Microstructures and photovoltaic properties of perovskite-type $\text{CH}_3\text{NH}_3\text{PbI}_3$ compounds. *Appl. Phys. Express* **2014**, *7*, 121601 doi:10.7567/APEX.7.121601.
35. Oku, T.; Ohishi, Y.; Ueoka, N. Highly (100)-oriented $\text{CH}_3\text{NH}_3\text{PbI}_3(\text{Cl})$ perovskite solar cells prepared with NH_4Cl using an air blow method. *RSC Adv.* **2018**, *8*, 10389–10395, doi:10.1039/c7ra13582c.
36. Stoumpos, C.C.; Malliakas, C.D.; Kanatzidis, M.G. Semiconducting tin and lead iodide perovskites with organic cations: Phase transitions, high mobilities, and near-infrared photoluminescent properties. *Inorg. Chem.* **2013**, *52*, 9019–9038, doi:10.1021/ic401215x.



© 2020 by the authors. Submitted for possible open access publication under the terms and conditions of the Creative Commons Attribution (CC BY) license (<http://creativecommons.org/licenses/by/4.0/>).